

Provided for non-commercial research and education use.
Not for reproduction, distribution or commercial use.



This article appeared in a journal published by Elsevier. The attached copy is furnished to the author for internal non-commercial research and education use, including for instruction at the authors institution and sharing with colleagues.

Other uses, including reproduction and distribution, or selling or licensing copies, or posting to personal, institutional or third party websites are prohibited.

In most cases authors are permitted to post their version of the article (e.g. in Word or Tex form) to their personal website or institutional repository. Authors requiring further information regarding Elsevier's archiving and manuscript policies are encouraged to visit:

<http://www.elsevier.com/authorsrights>



Polymer solar cells based on P3HT:PC₇₁BM doped at different concentrations of isocyanate-treated graphene



Daniel Romero-Borja^{a,b}, José-Luis Maldonado^{a,*}, Oracio Barbosa-García^a, Mario Rodríguez^a, Enrique Pérez-Gutiérrez^a, Rosalba Fuentes-Ramírez^b, Guadalupe de la Rosa^{b,*}

^a Centro de Investigaciones en Óptica A.P. 1-948, León, Guanajuato 37000, Mexico

^b Universidad de Guanajuato, Lascurain de Retana 5, Guanajuato, Gto. C.P. 36000, Mexico

ARTICLE INFO

Article history:

Received 12 September 2014

Received in revised form 26 November 2014

Accepted 24 December 2014

Available online xxx

Keywords:

SPFGraphene
Electron acceptors
Organic photovoltaics

ABSTRACT

In this work, we report the effect of the doping with solution-processable functionalized graphene (SPFGraphene) the active film of polymer solar cells (PSCs) under the bulk heterojunction (BHJ) structure. Cells were based on a poly (3-hexylthiophene) (P3HT) and [6,6]-phenyl C₇₁-butyric acid methyl ester (PC₇₁BM) blend. The SPFGraphene was blended with a P3HT:PC₇₁BM mixture (1:0.8 w/w) at different ratios: 0, 3, 6, 9, 12 and 15 wt.%. Device architecture was ITO/PEDOT:PSS/P3HT:PC₇₁BM:SPFGraphene/PFN/FM, where FM = Field's metal is an eutectic alloy (Bi/In/Sn: 32.5%, 51%, and 16.5%, respectively) with a melting point above 62 °C. FM was used as cathode and deposited by drop-casting in a vacuum-free process. We used the alcohol/water-soluble conjugated polymer, poly [(9,9-bis(3'-(N,N-dimethylamino)propyl)-2,7-fluorene)-alt-2,7-(9,9-dioctylfluorene)] (PFN) as an electron transport layer (ETL). The best results were obtained with 6 wt.% of SPFGraphene: a short-circuit current density (J_{sc}) of 7.20 mA cm⁻², an open-circuit voltage (V_{oc}) of 0.560 V, a fill factor (FF) of 0.53, and a power conversion efficiency (PCE) of 2.15% were reached. This means an increase of ~59% in comparison with the PCE of undoped devices (0 wt.% of SPFGraphene). Our reported PCE is larger than those of previous reports using similar materials and graphene in the active layer. The SPFGraphene can be well dispersed with the P3HT and PC₇₁BM to form a homogeneous solution, which could improve exciton dissociation as well as provides the transport pathway of the electron species. Additionally, a statistical study is also discussed for the photovoltaic (PV) parameters at different SPFGraphene contents.

© 2014 Elsevier B.V. All rights reserved.

1. Introduction

Polymer solar cells (PSCs) are a promising cost-effective alternative for solar energy utilization. They have some advantages with respect to their inorganic counterparts, such as light weight, flexibility and are much less expensive [1]. The plastic nature of semiconducting polymers makes them excellent candidates for use in optoelectronic devices fabricated on flexible substrates; besides, they can be manufactured at normal room conditions [2]. Nowadays, PSCs provide a great possibility for a facile and environmentally friendly manufacturing method as well as power conversion efficiency (PCE) that has reached more than 9% [3–5]. The most frequently studied PSCs are fabricated under the

bulk-heterojunction (BHJ) approach and based on P3HT as the donor and PC₆₁BM as the acceptor, the reported PCE ranges from 2 to 6.5% [6]. The best efficiencies have been reached through thickness optimization of both hole and electron transport layers (HTL and ETL, respectively) and under extensive study of the surface roughness of several metal electrodes, the largest efficiency for PSCs based on P3HT:PC₆₁BM has been reported of 6.5% [7,8].

Fabrication of BHJ PSCs always implies certain problems, such as structural traps, isolated domains, and incomplete pathways in the percolation network [9]; these problems lead to inefficient transport of charge carriers to the electrodes and a low energy conversion. Therefore, it is extremely important to increase the interfacial area between the acceptor and donor (acceptor/donor), where charge carriers can dissociate and generate continuous pathways that enable them to reach the electrodes before recombination occurs. Different donor and acceptor materials have been synthesized and widely studied in order to obtain more stable materials, better HOMO/LUMO matching, wider and

* Corresponding authors. Tel.: +52 477 441 4200.

E-mail addresses: jlmr@cio.mx (J.-L. Maldonado), delarosa@ugto.mx (G. de la Rosa).

stronger light absorption. The acceptor materials have been studied to a lesser extent compared to donors; materials other than PCBM can be explored for use as acceptors [10]. Carbon based nanomaterials such as carbon nanotubes and graphene have gained considerable interest because of their potential use as multifunctional compounds and wide range of applications in different kinds of devices [11]. Since its discovery, the two-dimensional planar structure of graphene has been of great interest for different applications [12]. Graphene shows excellent electronic properties such as high mobility [13] that makes it an excellent candidate as acceptor in different OPV cells [14]. Thus, pristine graphene displays better electron-transport properties than PCBM but some factors such as insolubility and impurities complicate the use of graphene in device fabrication under solution-based process [11,14,15].

Soluble graphene has been obtained by an oxidation step (graphene oxide, GO) and a subsequent functionalization (SPFGraphene). Graphene has been used in BHJ solar cells as: (i) acceptor material in polymer:graphene based devices, (ii) doping material in polymer:fullerene mixture, and (iii) structural scaffold to support small molecules [14]. However, by using graphene, the overall PSC efficiency is rather moderate and few reports exist for PSC based on P3HT [14]. For instance, graphene as acceptor material in P3HT:SPFGraphene:MDMO-PPV (10:1:1.5 w/w) and P3HT:SPFGraphene:P3OT (10:1:1 w/w) active layers was investigated by Wang et al. [15] and the obtained PCE values were 1.51% and 1.12%, respectively; the structures of the BHJ solar cells used were ITO/PEDOT:PSS/P3HT:SPFGraphene:MDMO-PPV/LiF/Al and ITO/PEDOT:PSS/P3HT:SPFGraphene:P3OT/LiF/Al, the PCE reported with P3HT:SPFGraphene:MDMO-PPV (1.51%) as active layer, as far as is known, is the highest reached value until now [14,15]. Other reports have considered a mixture of P3HT:PC₆₁BM (1:1 w/w) with 10 wt.% of SPFGraphene as active layer in a device with the structure ITO/PEDOT:PSS/P3HT:PC₆₁BM:SPFGraphene/LiF/Al and the reported PCE was of 1.4% [16]. Graphene was also studied as structural scaffold by Wang et al. [17] in graphene-organic hybrid wire (*N,N*-dioctyl-3,4,9,10-perylenedicarboximide (PDI)-graphene (G)), P3HT:G-PDI hybrid wires (1:0.5 w/w) were used as active layer in BHJ solar cells; the structure of the device was ITO/PEDOT:PSS/P3HT:G-PDI/LiF/Al, yielding a PCE of 1.04%. In these reports, the Hummers method [18] was used during the oxidation step in which the graphite is treated with concentrated sulfuric acid, sodium nitrate and potassium permanganate (H₂SO₄, NaNO₃, KMnO₄). However, the obtained oxidized shows disruptions in both the basal plane and the edges, which significantly reduces its electronic properties. An improved method was developed by Marcano et al. [19], in which it is excluded the NaNO₃ and included H₃PO₄ mixed with H₂SO₄. This method improves the efficiency of the oxidation process and disrupts the basal plane of the graphite less than Hummers method and its electronic properties can be recovered more easily. On the other hand, Wood's and Field's metals (WM and FM, respectively) have been reported as convenient substitutes of aluminum as the cathode of the PSCs for easy, economical and fast evaluation [20,21]. These metals have melting points below 80 °C, which permit them to be applied without a vacuum chamber.

Here, we report the fabrication and performance of polymer:fullerene:SPFGraphene active layer in PSCs with a bulk hetero-junction (BHJ) structure. Different SPFGraphene concentrations were added to the P3HT:PC₇₁BM mixture. The improved method for the preparation of graphene oxide (GO) developed by Marcano et al. [19] used in this work produced a well-oxidized, planar graphitic material, with few defects induced during the oxidation step. The entire PSCs manufacturing process was performed under ambient conditions and FM was used as a cathode instead of the most common Al. Thus, fabrication of the

devices was easy and fast, without the need of a vacuum step. The PCE achieved with such devices was significantly larger than those previously reported, where similar materials in the active layer were used [14,16]. Averages and standard deviation values of J_{SC} , V_{OC} , FF , and PCE were obtained from 24 fabricated devices in order to carry out a statistical study.

2. Experimental

2.1. Materials

Electron donor material P3HT and electron acceptor PC₇₁BM were purchased from Rieke Metals, Inc. and American Dye Source, Inc., respectively, and used as received. The PEDOT:PSS (Clevios P AI4083) was obtained from Heraeus-Clevios and PFN [3] was purchased from 1-Material, Inc. ITO/glass substrates (~10 Ω/square) and Field's metal were acquired from Delta Technologies and Rotometals, respectively. Fig. 1 shows the molecular structure of PEDOT:PSS, PC₇₁BM, SPFGraphene, P3HT and PFN. Diethyl ether (99%) and chloroform (99.8%) were purchased from Karal. *N,N*-dimethylformamide (99.8%), phenyl isocyanate (98%), and 1,2-dichlorobenzene (99%) were acquired from Aldrich.

2.1.1. Preparation of graphene oxide

Graphite was oxidized using the method reported by Marcano et al. [19]. A solution of concentrated H₂SO₄/H₃PO₄ (360:40 ml) was added to a mixture of graphite powder (3.0 g) and KMnO₄ (18.0 g), producing a slight rise in temperature (c.a. 40 °C). Then, the reaction was heated to 50 °C and stirred for 12 h. The resultant mixture was poured onto ice (c.a. 400 ml) with 30% H₂O₂ (3 ml); the color of the solution turned from dark brown to yellow. The reaction mixture was then allowed to settle overnight to remove large particles. Mixture was centrifuged (4000 rpm for 10 min), and the liquid was eliminated. In order to remove undesired elements, the remaining solid material was purified by addition of an aqueous solution of 3 wt.% H₂SO₄/0.5 wt.% H₂O₂ (200 ml), stirred, ultrasonicated (30 min), and centrifuged (4000 rpm/10 min). This procedure was repeated three times. In order to remove acidity, the material was poured and stirred three times in HCl (200 ml, 3 wt.%) and twice in deionized water (200 ml). Supernatant was removed in each stage following centrifugation (4000 rpm/10 min). After the washing procedure, the remaining material was coagulated in diethyl ether (200 ml). Finally, through a drying process graphene oxide was obtained.

2.1.2. Functionalization of graphene oxide

Functionalization process of the graphene oxide was performed by suspending dried graphene oxide (500 mg) in anhydrous *N,N*-dimethylformamide (DMF, 50 ml), and treated with phenyl isocyanate (45 ml) for a week. Then, the reaction mixture was added drop-wise into 1,2-dichlorobenzene (DCB, 50 ml) and centrifuged at 1000 rpm for 10 min. The upper solution was poured into CHCl₃ (100 ml) and centrifuged at 10,000 rpm to collect the deposit at the bottom. This procedure was repeated twice to get the purified functionalized graphene (SPFGraphene) [22].

2.2. Characterization of GO and SPFGraphene

Elemental analysis for the SPFGraphene was carried out on a Thermo Finnigan Flash EA 1112 elemental microanalyzer. For spectroscopic characterization of the synthesized materials, Raman and FT-IR spectra with a Raman microscope (Renishaw inVia) and Fourier transforms infrared spectrometer (Spectrum One PerkinElmer) were collected. The absorption spectra were measured in a Lambda 900 UV-vis-NIR spectrometer. Thickness

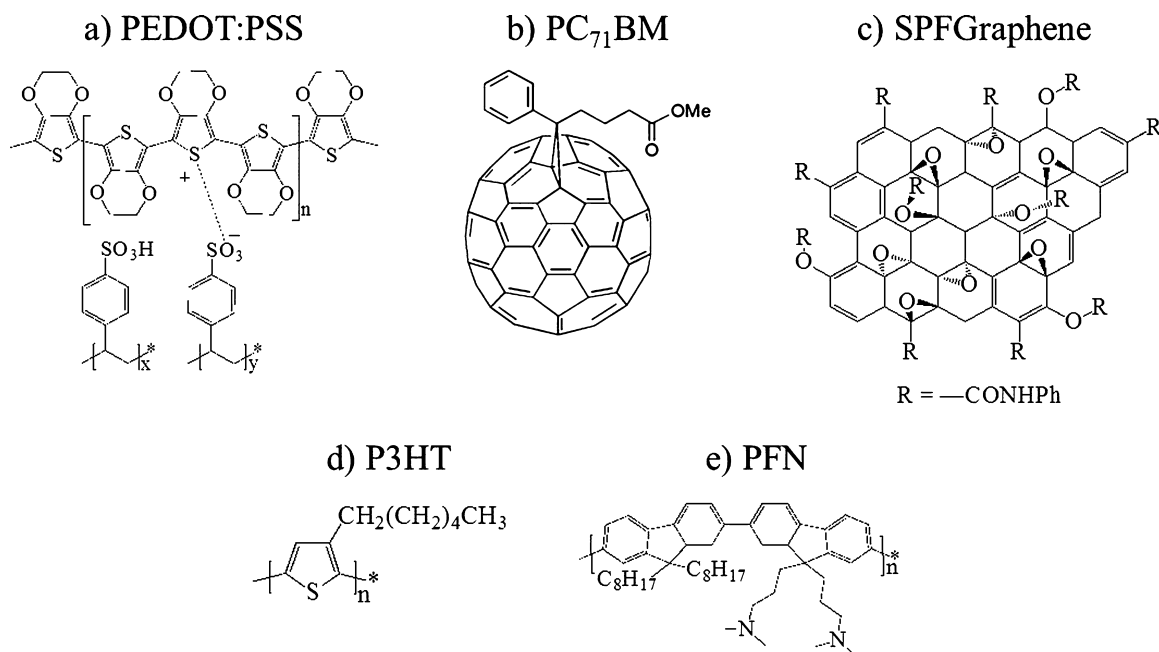


Fig. 1. Chemical structures of the organic compounds used in this work.

and morphology films were obtained using an atomic force microscope (AFM, easyscan2 from Nanosurf), operating in contact mode. The silicon cantilever was 450 μm long with a force constant of 0.2 N/m.

2.3. Fabrication of PSCs and testing

Polymer solar cells (PSCs) based on SPFGGraphene and P3HT:PC₇₁BM mixture were fabricated using a common process under ambient conditions [20,21,23]. Prior to device fabrication, the indium tin oxide (ITO) coated glass substrates were sequentially cleaned in detergent, de-ionized water, acetone and isopropanol. The hole-injection buffer layer of poly(ethylene dioxythiophene) with polystyrene sulfonic acid (PEDOT:PSS) was spin-coated on the ITO-coated glass substrate at 5000 RPM for 60 s (~ 40 nm of thickness), the PEDOT:PSS-coated substrates were thermally treated for 10 min at 120 °C in a hot plate. The P3HT:PC₇₁BM mixture (1:0.8 w/w) was dissolved in chlorobenzene and stirred for 12 h at 40 °C under normal conditions. Separately, regarding the different SPFGGraphene concentrations, small amount of the prepared solution (15 mg ml⁻¹ in chlorobenzene) in volumes of 0, 15, 30, 45, 60 and 75 μl were added to six vials with the P3HT:PC₇₁BM combination and sonicated for 1 h to obtain the P3HT:PC₇₁BM:SPFGGraphene mixtures with different SPFGGraphene weight ratios (0, 3, 6, 9, 12 and 15 wt.%, respectively, with respect to P3HT). The resultant P3HT:PC₇₁BM:SPFGGraphene solutions were spin coated onto PEDOT:PSS-coated substrates (2500 rpm, ~ 100 nm of thickness). Then, these films were subjected to thermal annealing for 10 min at 160 °C in a hot plate in order to remove some functional groups from SPFGGraphene and partially recover the planar structure of graphene and its conductivity as described by Liu et al. [24]. The PFN [3] interlayer material was dissolved in methanol (concentration: 2 mg ml⁻¹) under the presence of a small amount of acetic acid. The resulting mixture was diluted with methanol (1:5 v/v) and spin-coated on top of active layer. Finally, Field's metal pellets were melted on a hotplate at 95 °C. The melted eutectic alloy was deposited drop-wise on the patterned substrate, the active area was 0.03 cm². For statistical purposes, a total of 24 devices (4 for each SPFGGraphene content)

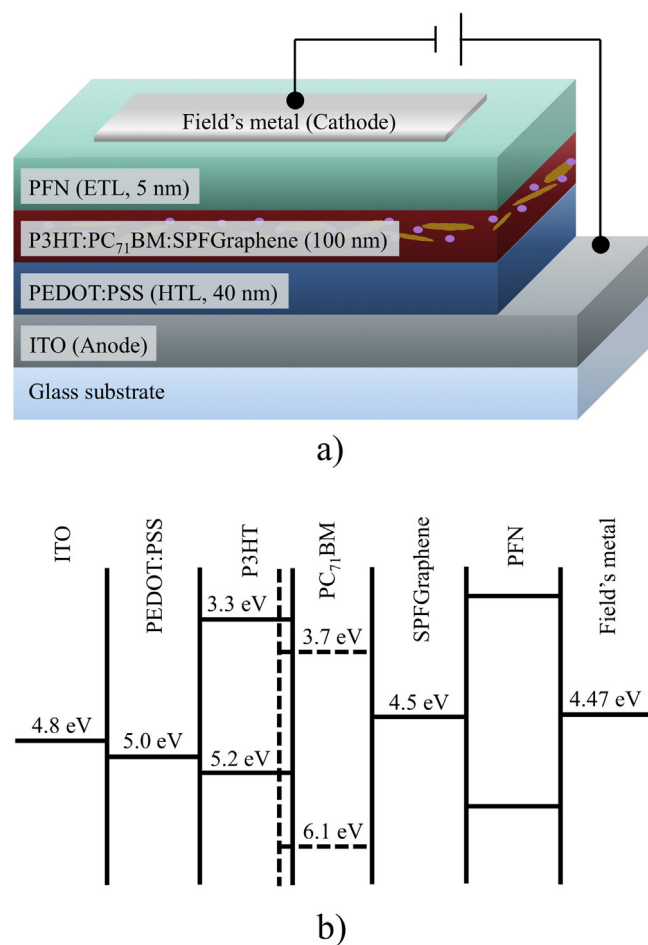


Fig. 2. (a) Schematic architecture of the devices based on P3HT:PC₇₁BM:SPFGGraphene as active layer and, films thicknesses. (b) Schematic diagram of the energy levels for the fabricated devices.

were fabricated. Fig. 2 shows the configuration of the fabricated PSCs and the schematic diagram of the energy levels for the devices.

Determination of PCE was performed according to $PCE = (FF \times V_{OC} \times J_{SC})/P_{in}$, where P_{in} is the incident light power. The fill factor (FF) is determined according to $FF = (V_m \times J_m)/(V_{OC} \times J_{SC})$, where V_m and J_m are the voltage and the current density in the maximum power point of the J - V curve in the fourth quadrant. Current density–voltage (J - V) of the photovoltaic devices were measured using a Keithley 2400 source measure unit and a halogen lamp calibrated with an Oriel reference cell at 100 mW cm^{-2} (AM1.5 conditions).

3. Results and discussion

Fig. 3 shows Raman spectra of graphite and GO. The Raman spectrum of the graphite, as expected, displays a prominent G peak at $\sim 1580 \text{ cm}^{-1}$ [25], corresponding to the first-order scattering of the E_{2g} mode. In the Raman spectrum of GO, the G band is broadened and shifted to $\sim 1595 \text{ cm}^{-1}$. In addition, the D band at $\sim 1315 \text{ cm}^{-1}$ becomes prominent, confirming the lattice distortions and indicating the reduction in size of the in-plane $C(\text{sp}^2)$ domains, most likely due to the extensive oxidation [26]. In order to know the oxidation degree of graphite, D/G peaks ratio ($C(\text{sp}^3)/C(\text{sp}^2)$ ratio) was evaluated. This ratio for graphite was 0.27 in contrast with 1.26 for graphite oxide that confirms the lattice distortions due to the oxidation step. The D peak is associated with the existence of defects; the lower intensity of D peak corresponds to fewer defects of the graphene layer [27].

Fig. 4 shows the FT-IR spectrum of GO and SPFGGraphene. The functionalization of graphene oxide leads to the derivatization of both the edge carboxyl and surface hydroxyl functional groups via formation of amides [28] or carbamate esters [29], respectively. The chemical changes occurring upon treatment of GO with phenyl isocyanate can be observed by FT-IR spectroscopy as both GO and its isocyanate-treated derivatives display characteristic IR spectra. The main absorption bands in the FT-IR spectrum of GO correspond to vibrational deformation of the $\text{C}=\text{O}$ carbonyl at 1733 cm^{-1} , $\text{O}-\text{H}$ at 3395 cm^{-1} , $\text{C}-\text{OH}$ at 1226 cm^{-1} , and the $\text{C}-\text{O}$ at 1056 cm^{-1} [30].

Upon treatment with phenyl isocyanate, the $\text{C}=\text{O}$ stretching vibration at 1733 cm^{-1} in GO becomes hidden by the appearance of a strong absorption at 1702 cm^{-1} that can be attributed to the carbonyl stretching vibration of the carbamate esters in SPFGGraphene. The new stretch at 1648 cm^{-1} can be assigned to an amide carbonyl-stretching mode (the so-called Amide I vibrational stretch). The new band at 1533 cm^{-1} can be originated from either amides or carbamate esters and corresponds to

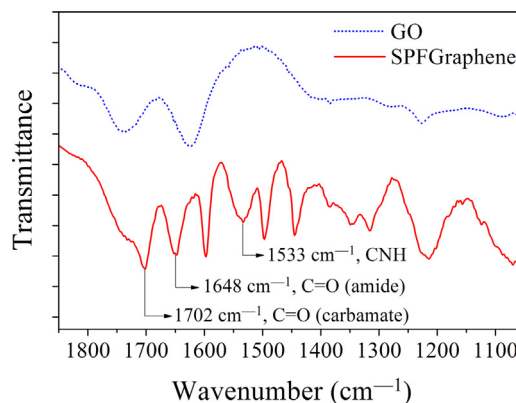


Fig. 4. FT-IR spectra of graphene oxide (GO) and solution-processable functionalized graphene (SPFGGraphene).

the coupling of the $\text{C}-\text{N}$ stretching vibration with the CHN deformation vibration (the so-called Amide II vibration) [31]. The FT-IR spectra of SPFGGraphene do not contain signals associated with the isocyanate group ($\sim 2263 \text{ cm}^{-1}$), indicating that the treatment of GO with phenyl isocyanate results in chemical reactions and not mere absorption/intercalation of the organic isocyanate. The atomic ratio between carbon and nitrogen (C/N) in SPFGGraphene can be used to calculate an approximated functionalization degree. According to elemental analysis, the weight fractions of N, C, and H of the SPFGGraphene were determined to be 5%, 58%, and 3%, respectively. Thus, C/N ratio was calculated as 11.6, which is consistent with previous values [22].

Fig. 5 shows the UV/vis/NIR absorption spectra of the P3HT:PC₇₁BM:SPFGGraphene (SPFGGraphene content: 0 and 6 wt.%) films and SPFGGraphene in chloroform. The absorption band of P3HT:PC₇₁BM is in the 450–650 nm range. The P3HT:PC₇₁BM:SPFGGraphene films have almost the same absorption range and displays the same peak as that of the P3HT:PC₇₁BM mixture because there is not absorption of SPFGGraphene in the range of 300–800 nm. Hence, there is not significant ground state interaction between SPFGGraphene and P3HT:PC₇₁BM mixture [32].

Fig. 6 shows the J - V plots under illumination of the ITO/PEDOT:PSS/P3HT:PC₇₁BM:SPFGGraphene/PFN/FM devices for all SPFGGraphene contents. The PV parameters: V_{OC} , J_{SC} , FF and PCE , are extracted from these curves and values are summarized in Table 1. It is important to mention that for OPVs devices fabricated under the BHJ approach, the upper limit of V_{OC} correlates with the energy difference of the electron donor HOMO and the electron acceptor LUMO levels. However, the fabrication process conditions, room

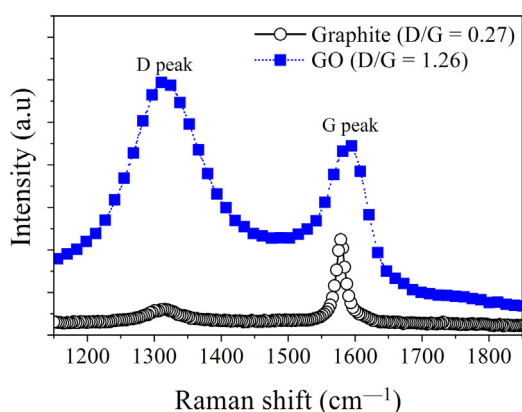


Fig. 3. Raman spectra of graphite and GO using 514 nm laser excitation.

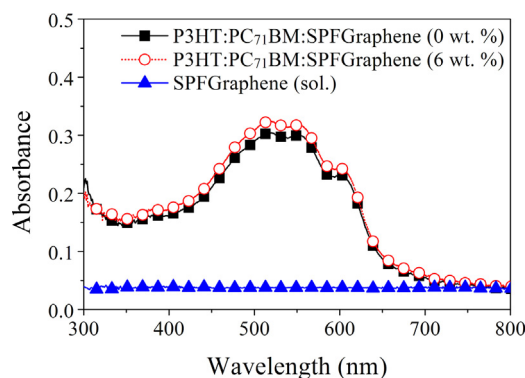


Fig. 5. UV/vis/NIR absorption spectra of P3HT:PC₇₁BM:SPFGGraphene films with SPFGGraphene content: 0 and 6 wt.% (filled squares and open circles, respectively), and SPFGGraphene solution in chloroform (filled triangles).

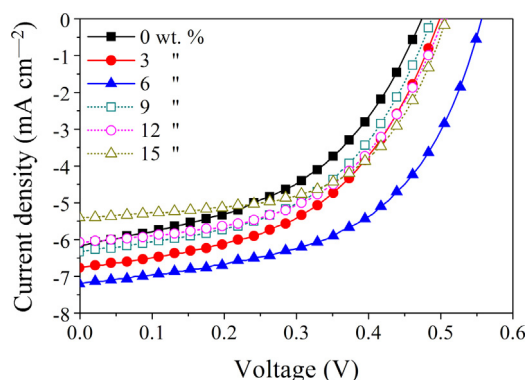


Fig. 6. Current density–voltage (J – V) characteristics of the photovoltaic devices based on P3HT:PC₇₁BM:SPFGraphene films.

ambient situations, the used buffer layers (Hole Transport Layer (HTL) and Electron Transport Layer (ETL)), the weight ratios and concentration of donor and acceptor materials, film thicknesses, film morphology, etc., are a few (among many) factors that affect the V_{oc} value and the other PV parameters [2,9,10].

We achieved the largest PCE value of 2.15%, from solar devices with 6 wt.% of SPFGraphene; which not only acts as electron acceptor, but also provides more polymer/graphene sites for better exciton dissociation as described by Liu et al. [16], they reported photovoltaic devices fabricated under similar architecture as the one used in this work (ITO/PEDOT:PSS/P3HT:PC₆₁BM:SPFGraphene/LiF/Al). Their best PCE value was of 1.4% using a P3HT:PC₆₁BM (1:1 w/w) mixture with 10 wt.% of SPFGraphene. As observed, we obtained higher PCEs values using less content of SPFGraphene (in Ref. 15, a 10% of SPFGraphene was also used), perhaps due to the oxidation method used during the synthesis of SPFGraphene an also, because of the use of PC₇₁BM instead of PC₆₁BM; the different ETL (PFN) and cathode (FM) could also play a role for this PCE enhancement, some details regarding these last three issues will briefly comment in a below paragraph. Hummers method was used in reports mentioned previously for the SPFGraphene [15–17]; during the oxidation process defects in the planar structure of graphite and functionalities of epoxy, alcohol and carboxylic groups are created. Herein, we used an improved oxidation method developed by Marcano et al. [19] in which a well-oxidized material was obtained allowing greater separation of the distance between the graphite layers. Besides, this method generates fewer defects (compared with Hummers method [18]) in the planar structure of the material then allowing subsequent recover of their conductive properties.

As previously commented in the introduction section, graphene has been used in BHJ solar cells as: (i) acceptor material in polymer:graphene based devices, (ii) doping material in polymer:fullerene mixture, and (iii) structural scaffold to support small [14]. For instance, graphene as acceptor material in P3HT:SPFGraphene:MDMO-PPV (10:1:1.5 w/w) and

Table 1

Active layer roughness (AFM measurements) and best PV parameters for devices with ITO/PEDOT:PSS/P3HT:PC₇₁BM (1:0.8 w/w):SPFGraphene ($X = \text{wt.}\%$)/PFN/FM architecture.

SPFGraphene ($X = \text{wt.}\%$)	Roughness (nm)	J_{sc} (mA cm^{-2})	V_{oc} (V)	FF	PCE (%)
0	6	6.17	0.472	0.46	1.35
3	7	6.77	0.494	0.50	1.67
6	6	7.20	0.560	0.53	2.15
9	9	6.33	0.483	0.51	1.55
12	11	6.07	0.505	0.52	1.58
15	21	5.40	0.505	0.58	1.57

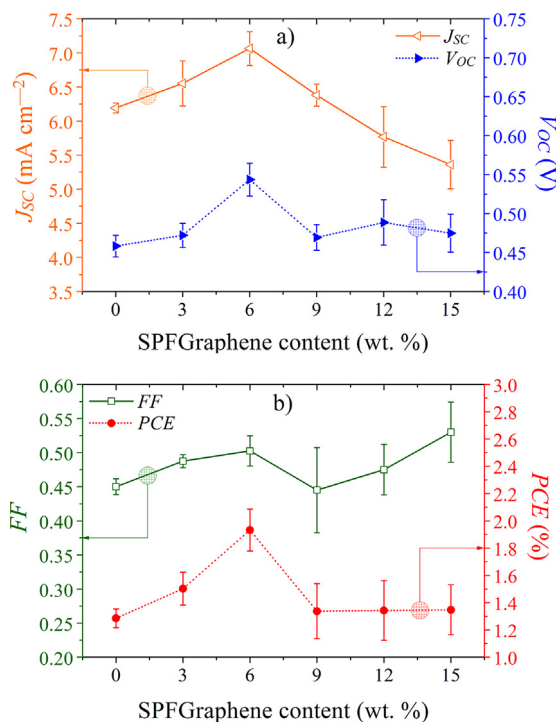


Fig. 7. Dependence of (a) J_{sc} and V_{oc} , and (b) the FF and PCE with different SPFGraphene content ($\mu \pm \sigma$).

P3HT:SPFGraphene:P3OT (10:1:1 w/w) active layers was studied by Wang et al. [15] with a PCE values of 1.51% and 1.12%, respectively, under the configurations ITO/PEDOT:PSS/P3HT:SPFGraphene:MDMO-PPV/LiF/Al and ITO/PEDOT:PSS/P3HT:SPFGraphene:P3OT/LiF/Al. Graphene has been also studied as structural scaffold by Wang et al. [17] in graphene–organic hybrid wire (*N,N*-dioctyl-3,4,9,10-perylenedicarboximide (PDI)-graphene (G)), here, P3HT:G-PDI hybrid wires (1:0.5 w/w) were employed as active layer in BHJ devices with a general structure: ITO/PEDOT:PSS/P3HT:G-PDI/LiF/Al, yielding a PCE of just 1.04%.

Regarding our results, there are other three differences in comparison with the previous mentioned reports: (a) the PCBM acceptor material used, (b) the cathode and deposition technique and (c) the ETL. PC₇₁BM has better absorption in the visible region compared to PC₆₁BM, this can lead to improved light-harvesting in OPVs. Also LiF/Al was deposited in a vacuum evaporation chamber while in our work the Field's metal was deposited under ambient conditions, which significantly facilitates fabrication. Finally, herein, a water/alcohol soluble PFN polymer as electron transport layer was deposited via solution-technique [3]. Further, the cathode used in this work (FM) allowed us reaching very acceptable FF values ranging from 0.46 to 0.58 (Table 1). The work function of the FM was estimated by a set of experiments to analyze the energy barriers of the Schottky junctions of this metal

Table 2

Averages \pm standard deviations for PV parameters of devices based on P3HT:PC₇₁BM (1:0.8 w/w):SPFGraphene ($X = \text{wt.}\%$) as active layer.

SPFGraphene ($X = \text{wt.}\%$)	J_{sc} (mA cm^{-2})	V_{oc} (V)	FF	PCE (%)
0	6.19 ± 0.07	0.458 ± 0.014	0.45 ± 0.01	1.29 ± 0.07
3	6.55 ± 0.33	0.472 ± 0.016	0.49 ± 0.01	1.50 ± 0.12
6	7.07 ± 0.25	0.544 ± 0.021	0.50 ± 0.02	1.93 ± 0.15
9	6.38 ± 0.16	0.469 ± 0.017	0.45 ± 0.06	1.34 ± 0.20
12	5.77 ± 0.46	0.489 ± 0.029	0.48 ± 0.04	1.34 ± 0.22
15	5.36 ± 0.36	0.475 ± 0.024	0.53 ± 0.04	1.35 ± 0.18

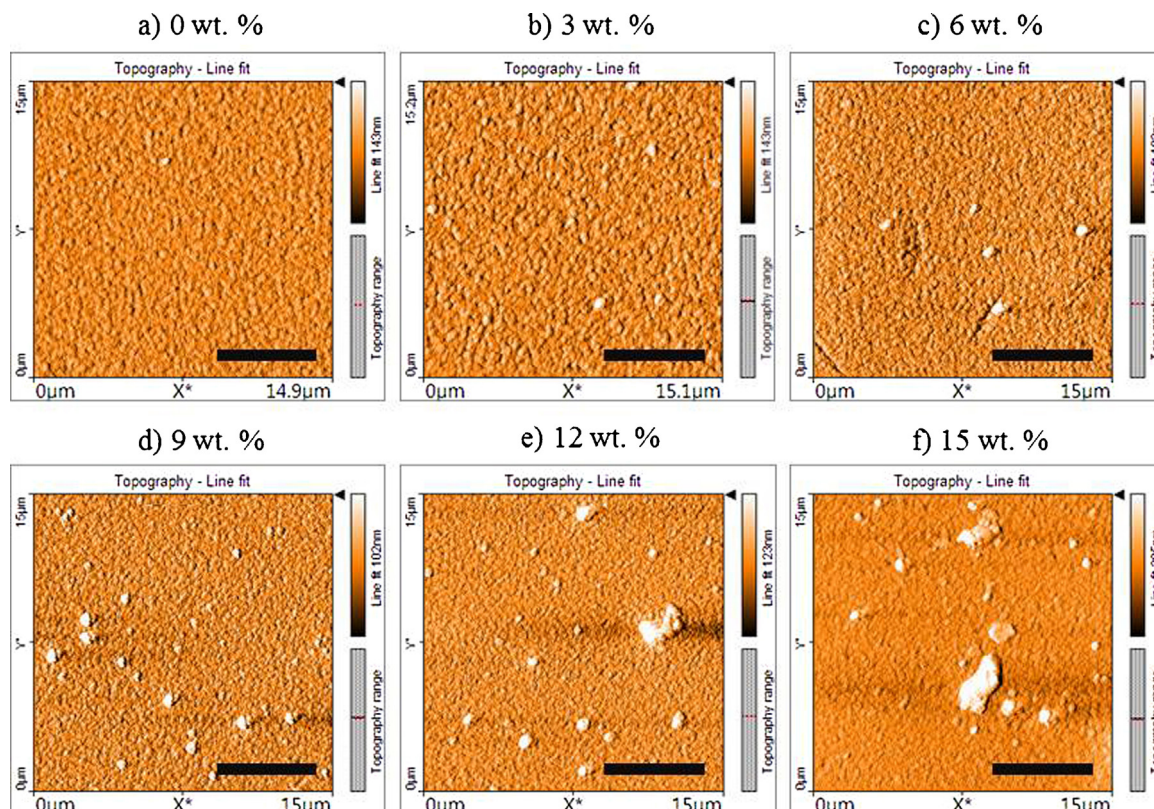


Fig. 8. Roughness of P3HT:PC₇₁BM:SPFGraphene active layers with different ratios of SPFGraphene (scale bar = 5 μm).

with the semiconductor polymer P3HT and was reported as 4.47 eV [33], close to aluminum work function (4.3 eV) [34]. The work function of graphene often reported is 4.5 eV [14–16]. For SPFGraphene it is different; however, after thermal annealing treatment (of the functionalized graphene) and the subsequent recovery of its planar structure, the work function of SPFGraphene could be closer to the work function of FM electrode (4.47 eV) [24] and will form the transport pathway of LUMO–fullerene–graphene–FM for the electronic mobility. Fig. 2b shows the energy level diagram of the charge transfer process.

Fig. 7 shows the dependence of the PV parameters with different SPFGraphene contents. Averages and standard deviations ($\mu \pm \sigma$) for these parameters (J_{SC} , V_{OC} , FF and PCE) were calculated using data of 4 devices per each SPFGraphene content (a total of 24 devices for this study) and are summarized in Table 2. It may be noticed that all device parameters are influenced by SPFGraphene contents in the mixtures. The J_{SC} , V_{OC} and PCE have a behavior in which first increase and then decrease (Fig. 7). Particularly, the PCE in the SPFGraphene-doped devices increase from 1.35% (SPFGraphene 0wt.%) to 2.15% mainly due to the higher J_{SC} (7.20 mA cm⁻²) achieved in the doped cells with 6 wt.% SPFGraphene, which represents an increase in the PCE of ~59%.

In the undoped device (0 wt.% of SPFGraphene), the photo-generated excitons were dissociated at the P3HT:PC₇₁BM interface, and the electrons are transported from fullerenes to the top contact (FM) across the thin PFN interlayer. The incorporation of the SPFGraphene in the active layer provides additional pathways for the electron transport between the fullerenes and SPFGraphene, suppressing charge recombination [35]. The increase of J_{SC} is mainly due to a more efficient charge carrier transport through the SPFGraphene pathways [36]. However, trapping and recombination of charge carriers occurs at high SPFGraphene contents due to aggregates formation on film surface (Fig. 8), which reduces mobility and then J_{SC} value. On the other hand, the

addition of SPFGraphene (after thermal annealing) could improve the V_{OC} value because its work function (~4.5 eV) [15] can act as a bridge between the energy levels of P3HT and PC₇₁BM. However, also at high contents of SPFGraphene V_{OC} decreases, probably due to the stacks formation in between SPFGraphene layers.

Fig. 8 shows a comparison of AFM images of the active layers with different ratios of SPFGraphene. As the SPFGraphene content further increases, for example 15 wt.%, aggregation of the SPFGraphene occurs, as a result of an excessive amount of SPFGraphene in the P3HT matrix [37]. As mentioned above, this fact could have an unwanted effect on exciton generation and charge separation/transport in the active layer causing a decrease in the J_{SC} value (Fig. 9).

Fig. 9 shows the behavior of the surface roughness, J_{SC} and FF as a function of SPFGraphene content. The roughness curve shows that blend morphology is almost the same for films with 0, 3 and 6 wt.% of SPFGraphene, and then increases at higher SPFGraphene contents of 9 to 15 wt.% mainly due to SPFGraphene aggregates.

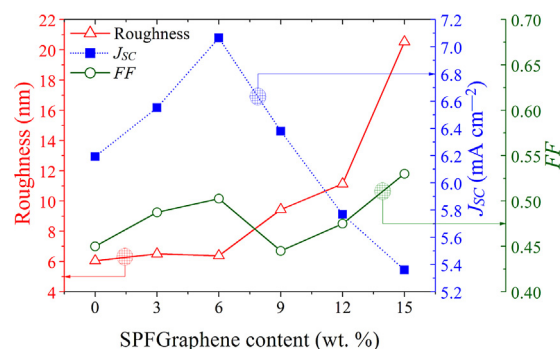


Fig. 9. Behavior of surface roughness, J_{SC} , and FF with respect to the amount of SPFGraphene.

Table 3
Results of one-way ANOVA and post hoc test.

Photovoltaic (PV) Parameter	Normality Shapiro–Wilk test	Homogeneity Levene test	ANOVA	Average comparisons Tukey post hoc test Best group(s)
J_{sc}	0.360	0.076	0.000	3 and 6 wt.%
V_{oc}	0.017	0.446	0.000	6 wt.%
FF	0.776	0.003	0.032 (0.065)	–
PCE	0.113	0.168	0.000	6 wt.%

The improvement of FF can be attributed to the increases of roughness on films when SPFGGraphene contents increases [24]. That is, a larger contact area between the active layer and PFN/FM top contact. At high SPFGGraphene amount, large stacks formation can be occur on film surface causing electrical short circuits; this likely explains the decrease in V_{oc} . As a consequence of the mentioned above, the maximum PCE has been obtained with 6 wt.% SPFGGraphene, when aggregates are not well formed.

It should be noticed that V_{oc} reaches a maximum of 0.544 ± 0.021 V with 6 wt.% of SPFGGraphene content. J_{sc} of the undoped devices (SPFGGraphene 0 wt.%) is 6.19 ± 0.07 mA cm⁻². Upon adding SPFGGraphene, J_{sc} increases reaching a maximum value of 7.07 ± 0.25 mA cm⁻², also with 6 wt.% SPFGGraphene, and then decays to 6.22 ± 0.61 mA cm⁻² with 15 wt.% ratio (Fig. 7(a)). The maximum average fill factor was yielded at 15 wt.% SPFGGraphene as 0.53 ± 0.04 .

In order to compare, from a statistical point of view, the average values between the different SPFGGraphene contents, one-way analysis of variance (ANOVA) and a post hoc test were used [38]. The assumptions required for ANOVA are: (i) independence of observations, (ii) the dependent variable (J_{sc} , V_{oc} , FF and PCE) is normally distributed, and (iii) the variances in each group are equal. Table 3 shows the p -values of statistical analysis for each PV parameters (statistical significance was set at p -value <0.05). According to ANOVA results for J_{sc} , V_{oc} and PCE, we determined that there are significant differences between SPFGGraphene contents. The multiple average comparisons were carried out with Tukey post hoc test, and results confirmed that 6 wt.% SPFGGraphene is statistically different than each other SPFGGraphene contents. In the other hand, homogeneity of variances was violated in the case of FF, as determined by Levene's test (p -value = 0.003), so the Brown–Forsythe robust test for unequal variances was used. The results of Brown–Forsythe test revealed that for FF there are not statistically significant differences between SPFGGraphene contents (p -value = 0.065).

4. Conclusions

SPFGGraphene was successfully dispersed into a P3HT:PC₇₁BM (D:A) mixture solution in order to fabricate photovoltaic devices by the process-solution technique. An efficiency of 2.15%, with $J_{sc} = 7.20$ mA cm⁻², $V_{oc} = 0.560$ V and FF = 0.53, was achieved with 6% of SPFGGraphene in ternary (D:A:SPFGGraphene) blends. This PCE value was superior in about 59% when compared to the undoped samples and, additionally, devices were fabricated with Field's metal as the cathode, which allow testing easily and quickly the performance of PV devices in a more practical way, without the need of sophisticated vacuum deposition equipment under vacuum free conditions. Further, the achieved efficiency was significantly superior to the reported by other authors using similar active materials and evaporated Al as cathode. We also reached the best PV parameters with a lesser amount of SPFGGraphene (6 wt.%) compared to previous works (10 wt.%). ANOVA test revealed that J_{sc} , V_{oc} and PCE average values obtained

with 6 wt.% SPFGGraphene are considerably different from the rest of the values.

Acknowledgments

This work was supported by CONACyT-SENER (Mexico) project 153094 and IER-UNAM (Mexico) through project CeMIE-Sol 207450/27 call 2013-02, Fondo Sectorial CONACyT-SENER-SUSTENTABILIDAD ENERGETICA. Daniel Romero-Borja wishes to thank CONACyT (218216) and Universidad de Guanajuato. We also acknowledge Centro de Investigaciones en Óptica (CIO) and Universidad de Guanajuato for financial support (UG-CIO 001/2014). Authors acknowledge Karina-Sánchez and M. Olmos for technical assistance.

References

- [1] N. Yeh, P. Yeh, Organic solar cells: their developments and potentials, *Renew. Sustainable Energy Rev.* 21 (2013) 421–431.
- [2] C.J. Brabec, N.S. Sariciftci, J.C. Hummelen, Plastic solar cells, *Adv. Funct. Mater.* 11 (2001) 15–26.
- [3] Z. He, C. Zhong, S. Su, M. Xu, H. Wu, Y. Cao, Enhanced power-conversion efficiency in polymer solar cells using an inverted device structure, *Nat. Photonics* 6 (2012) 591–595.
- [4] S. Liu, K. Zhang, J. Lu, J. Zhang, H.-L. Yip, F. Huang, Y. Cao, High-efficiency polymer solar cells via the incorporation of an amino-functionalized conjugated metallopolymer as a cathode interlayer, *J. Am. Chem. Soc.* 135 (2013) 15326–15329.
- [5] S.-H. Liao, H.-J. Jhuo, Y.-S. Cheng, S.-A. Chen, Fullerene derivative-doped zinc oxide nanofilm as the cathode of inverted polymer solar cells with low-bandgap polymer (PTB7-Th) for high performance, *Adv. Mater.* 25 (2013) 4766–4771.
- [6] M.T. Dang, L. Hirsch, G. Wantz, P3HT:PCBM best seller in polymer photovoltaic research, *Adv. Mater.* 23 (2011) 3597–3602.
- [7] S.-H. Lee, J.-H. Kim, T.-H. Shim, J.-G. Park, Effect of interface thickness on power conversion efficiency of polymer photovoltaic cells, *Electron. Mater. Lett.* 5 (2009) 47–50.
- [8] S.-H. Lee, D.-H. Kim, J.-H. Kim, G.-S. Lee, J.-G. Park, Effect of metal-reflection and surface-roughness properties on power-conversion efficiency for polymer photovoltaic cells, *J. Phys. Chem. C* 113 (2009) 21915–21920.
- [9] C.J. Brabec, S. Gowrisanker, J.J.M. Halls, D. Laird, S. Jia, S.P. Williams, Polymer-fullerene bulk-heterojunction solar cells, *Adv. Mater.* 22 (2010) 3839–3856.
- [10] H. Zhou, L. Yang, W. You, Rational design of high performance conjugated polymers for organic solar cells, *Macromolecules* 45 (2012) 607–632.
- [11] T. Kuila, S. Bose, A.K. Mishra, P. Khanra, N.H. Kim, J.H. Lee, Chemical functionalization of graphene and its applications, *Prog. Mater. Sci.* 57 (2012) 1061–1105.
- [12] K.S. Novoselov, A.K. Geim, S.V. Morozov, D. Jiang, Y. Zhang, S.V. Dubonos, I.V. Grigorieva, A.A. Firsov, Electric field effect in atomically thin carbon films, *Science* 306 (2004) 666–669.
- [13] Y. Gao, P. Hao, Mechanical properties of monolayer graphene under tensile and compressive loading, *Phys. E* 41 (2009) 1561–1566.
- [14] A. Iwan, A. Chuchmała, Perspectives of applied graphene: polymer solar cells, *Prog. Polym. Sci.* 37 (2012) 1805–1828.
- [15] J. Wang, Y. Wang, D. He, Z. Liu, H. Wu, H. Wang, P. Zhou, M. Fu, Polymer bulk heterojunction photovoltaic devices based on complex donors and solution-processable functionalized graphene oxide, *Solar Energy Mater. Solar Cells* 96 (2012) 58–65.
- [16] Z. Liu, D. He, Y. Wang, H. Wu, J. Wang, Graphene doping of P3HT:PCBM photovoltaic devices, *Synth. Met.* 160 (2010) 1036–1039.
- [17] S. Wang, B.M. Goh, K.K. Manga, Q. Bao, P. Yang, K.P. Loh, Graphene as atomic template and structural scaffold in the synthesis of graphene-organic hybrid wire with photovoltaic properties, *ACS Nano* 4 (2010) 6180–6186.
- [18] W.S. Hummers, R.E. Offeman, Preparation of graphitic oxide, *J. Am. Chem. Soc.* 80 (1958) 1339–1339.

- [19] D.C. Marcano, D.V. Kosynkin, J.M. Berlin, A. Sinitzskii, Z. Sun, A. Slesarev, L.B. Alemany, W. Lu, J.M. Tour, Improved synthesis of graphene oxide, *ACS Nano* 4 (2010) 4806–4814.
- [20] C. Salto, J.F. Salinas, J.L. Maldonado, G. Ramos-Ortíz, M. Rodríguez, M.A. Meneses-Nava, O. Barbosa-García, J.A. Del-Oso, M. Ortiz-Gutiérrez, Performance of OPVs cells with the eutectic alloy Wood's metal used as cathode and P3HT:PC₆₁BM blend as active layer, *Synth. Met.* 161 (2011) 2412–2416.
- [21] E. Pérez-Gutiérrez, J.L. Maldonado, J. Nolasco, G. Ramos-Ortíz, M. Rodríguez, U. Mendoza-De la Torre, M.A. Meneses-Nava, O. Barbosa-García, H. García-Ortega, N. Farfán, G. Granados, R. Santillan, E. Juaristi, Titanium oxide:fullerene composite films as electron collector layer in organic solar cells and the use of an easy-deposition cathode, *Opt. Mater.* 36 (2014) 1336–1341.
- [22] S. Stankovich, R.D. Piner, S.T. Nguyen, R.S. Ruoff, Synthesis and exfoliation of isocyanate-treated graphene oxide nanoplatelets, *Carbon* 44 (2006) 3342–3347.
- [23] J.F. Salinas, J.L. Maldonado, G. Ramos-Ortíz, M. Rodríguez, M.A. Meneses-Nava, O. Barbosa-García, R. Santillan, N. Farfán, On the use of Woods metal for fabricating and testing polymeric organic solar cells: an easy and fast method, *Solar Energy Mater. Solar Cells* 95 (2011) 595–601.
- [24] Z. Liu, Q. Liu, Y. Huang, Y. Ma, S. Yin, X. Zhang, W. Sun, Y. Chen, Organic photovoltaic devices based on a novel acceptor material: graphene, *Adv. Mater.* 20 (2008) 3924–3930.
- [25] Z. Sun, Z. Yan, J. Yao, E. Beitler, Y. Zhu, J.M. Tour, Growth of graphene from solid carbon sources, *Nature* 468 (2010) 549–552.
- [26] K.S. Subrahmanyam, S.R.C. Vivekchand, A. Govindaraj, C.N.R. Rao, A study of graphenes prepared by different methods: characterization properties and solubilization, *J. Mater. Chem.* 18 (2008) 1517–1523.
- [27] D.C. Elias, R.R. Nair, T.M.G. Mohiuddin, S.V. Morozov, P. Blake, M.P. Halsall, A.C. Ferrari, D.W. Boukhvalov, M.I. Katsnelson, A.K. Geim, K.S. Novoselov, Control of graphene's properties by reversible hydrogenation: evidence for graphane, *Science* 323 (2009) 610–613.
- [28] I.S. Blagbrough, N.E. Mackenzie, C. Ortiz, A.I. Scott, The condensation reaction between isocyanates and carboxylic acids. A practical synthesis of substituted amides and anilides, *Tetrahedron Lett.* 27 (1986) 1251–1254.
- [29] M.B. Smith, J. March, *March's Advanced Organic Chemistry: Reactions, Mechanisms, and Structure*, John Wiley & Sons Inc., New York, 2001, pp. 1182–1183.
- [30] T. Szabó, O. Berkesi, I. Dékány, DRIFT study of deuterium-exchanged graphite oxide, *Carbon* 43 (2005) 3186–3189.
- [31] F. Cataldo, Structural analogies and differences between graphite oxide and C₆₀ and C₇₀ polymeric oxides (fullerene ozopolymers), *Fullerenes Nanotubes Carbon Nanostruct.* 11 (2003) 1–13.
- [32] M.C. Wu, Y.Y. Lin, S. Chen, H.C. Liao, Y.J. Wu, C.W. Chen, Y.F. Chen, W.F. Su, Enhancing light absorption and carrier transport of P3HT by doping multi-wall carbon nanotubes, *Chem. Phys. Lett.* 468 (2009) 64–68.
- [33] J.C. Nolasco, G. Ramos-Ortiz, J.L. Maldonado, O. Barbosa-García, B. Ecker, E. von Hauff, Polymer/cathode interface barrier limiting the open circuit voltage in polymer:fullerene organic bulk heterojunction solar cells: a quantitative analysis, *Appl. Phys. Lett.* 104 (2014) 043308-1–043308-4.
- [34] H. Wu, F. Huang, Y. Mo, W. Yang, D. Wang, J. Peng, Y. Cao, Efficient electron injection from a bilayer cathode consisting of aluminum and alcohol-/water-soluble conjugated polymers, *Adv. Mater.* 16 (2004) 1826–1830.
- [35] S.K. Das, K. Ohkubo, Y. Yamada, S. Fukuzumi, F. D'Souza, Decorating single layer graphene oxide with electron donor and acceptor molecules for the study of photoinduced electron transfer, *Chem. Commun.* 49 (2013) 2013–2015.
- [36] J. Wang, Y. Wang, D. He, Z. Liu, H. Wu, H. Wang, Y. Zhao, H. Zhang, B. Yang, Composition and annealing effects in solution-processable functionalized graphene oxide/P3HT based solar cells, *Synth. Met.* 160 (2010) 2494–2500.
- [37] V. Shrotriya, J. Ouyang, R.J. Tseng, G. Li, Y. Yang, Absorption spectra modification in poly(3-hexylthiophene):methanofullerene blend thin films, *Chem. Phys. Lett.* 411 (2005) 138–143.
- [38] D.C. Montgomery, *Design and Analysis of Experiments*, fifth ed., Wiley, New York, 2000 Section 3–2.